RE-EXAMINATION OF DARK HALO CRATERS IN MULTI-BAND RADAR IMAGES OF THE MOON. Jun Du[1], Wenzhe Fa[1] and Takao Kobayashi[2], [1]Institute of Remote Sensing and Geographical Information System, Peking University, Beijing 100871, China (wzfa@pku.edu.cn). [2]Earth Planetary Science Department, Korea Institute of Geoscience and Mineral Resources, Daejeon 305-350, Korea.

Introduction: In radar images of the Moon, radar dark halo craters (RDHCs) are those craters with the presences of low-return ringed areas that extend ∼3-10 crater radii from their rims [1, 2]. Generally, radar echo strength (both same-sense-circular, SC, and opposite-sense-circular, OC) and CPR (circular polarization ratio, SC/OC) of the haloes are ∼2-6 dB lower than their surrounding terrain in 70 cm radar images. As radar wavelength decreases, dark haloes become less prominent (12.6 cm) and finally disappear (3.8 cm) [1]. RDHCs were thought to be induced by fine-grained ejecta and subsequently erased due to meteoroid bombardments, and previous investigations found that craters older than Early Imbrian no longer have distinctive dark-haloed features [1, 2]. Since radar echo from the lunar surface depends on the near-surface properties of the Moon, the formation mechanisms of RDHCs, and their behaviors with wavelength and variation with time, can provide important clues for impact cratering mechanism and postimpact surface modification process.

In previous studies, there is no systematical investigation about the spatial distributions of the RDHCs [1, 2]. In addition, though the origin of dark halo was attributed to the presence of fine-grained ejecta without rocks at wavelength scales, there is no direct evidence to support this hypothesis. In an attempt to solve the above problems, multi-band lunar radar images (12.6 and 70 cm Earth-based radar, Miniature Radio Frequency, Mini-RF, and Lunar Radar Sounder, LRS) in combination with the auxiliary multi-source datasets (cratering, elevation, rock abundance and ilmenite content map) were used in this study to discuss the spatial distribution characteristics and formation mechanisms of RDHCs.

Spatial Distribution Characteristics: An exhaustive search of RDHCs in the 12.6 cm Earth-based radar images was implemented for the first time. Fig. 1a shows the spatial distributions of 12.6 cm RHDCs (87), 70 cm RDHCs (275) [2], and ODHCs (optical dark halo craters, 191) [3, 4]. The number of the 12.6 cm RDHCs over maria is much larger than that over highlands regions, with a ratio of ∼3:1. When normalized to the areas over which RDHCs were counted, the relative ratio increases significantly to ∼10:1. In contrast, the spatial distribution of the 70 cm RDHCs is relatively uniform. ODHCs are concentrated along the margins between maria and highlands.

Given to the differences in penetration depth and sensitive scale of the scatterer, direct comparison of radar images at 12.6 and 70 cm can give information on near-surface properties of the Moon at different depths and scales. The discernible maria/highlands dichotomy in the distribution of the 12.6 cm RDHCs indicates that highlands RDHCs were prone to disappear than those over maria. This is because that the older highlands experienced more meteoroid bombardments than maria and that the 12.6 cm radar returns are dominated by shallower subsurface properties compared to 70 cm echoes. As a result, shallower fine-grained materials of 12.6 cm highlands dark haloes were easier to be erased during subsequent bombardments. Figs. 1b and 1c show the RDHC number as a function of relative cratering rate [5] along longitude and latitude (in a 5° bin). There is a weak signal that RDHC number increases with cratering rate, suggesting that the formation of RDHC is an exogenetic process and might only slightly correlate with the target properties. The clusters of ODHCs may indicate that the cryptomare regions subsequently overlaid by basin/crater bright ejecta [3], which are dominated by both exogenetic and endogenetic processes.

Formation Mechanisms: Considering potential parameters (low rock abundance and high ilmenite content) in the impact cratering process that could result in low-return radar echo, most of the previous studies ascribed the dark-haloed feature to fine-grained ejecta [1]. For example, Hermann crater (0.9°S, 57.3°W; 8 km) has radar dark haloes in both the 12.6 and 70 cm CPR images (Figs. 1d and 1e). The radius of the most distal dark halo is about four times the crater radius, and the averaged CPR in the dark-haloed region is ∼3 dB lower than that of its background terrain. As seen from rock distribution map derived from Diviner radiometer data (Fig. 1f) [6], the rock abundance of dark halo is only about half as that of the background. A significantly high ilmenite content around the crater is not observed in the TiO_2 map as expected (Fig. 1g). Therefore, ilmenite content is not the major factor for the dark halo craters in radar images.

The scattering mechanism of OC echo depends on radar incidence angle. Surface scattering dominates at smaller incidence angle (<35°), whereas volume scattering by rocks dominates at larger incidence angle (>35°). If RDHCs indeed result from low abundance of rocks, dark haloes should be more obvious at larger incidence

angle. To validate this, craters Hainzel A (40.5°S, 33.5°W; 55 km) and Bullialdus (20.7°S, 22.2°W; 60 km) with similar sizes and ages (Eratosthenian [7]) but different incidence angles (∼48° and ∼27°) were compared. For Hainzel A, the OC strength of the dark halo is ∼4 dB lower than its surrounding terrain, which is more obvious than the situation of Bullialdus with a contrast of only ∼2 dB. Since Bullialdus's distal ejecta and the surrounding mare region have similar topography, its dark halo in the OC image is too weak to be detected. This phenomenon indicates indirectly that the low rock abundance is most probably the major factor for RDHC.

Two ODHCs, Schickard R (44.1°S, 53.6°W; 5 km) and Alphonsus R (14.4°S, 1.9°W; 3 km) [8], were found to have radar dark haloes in Mini-RF images. This result shows that the volcanic geologic contexts can also be the scenarios for RDHC's formation in addition to fine-grained ejecta. However, though RDHC can have both impact and volcanic origins, the mechanism of the low radar return might be ascribed to the same radar scattering parameter, i.e., the low rock abundance.

LRS RDHC: In LRS surface image with a wavelength of 60 m [9], most of the large craters have dark haloes. Because lunar surface is depleted in blocks at tens of meters scale [6], radar return of LRS depends largely on wavelength-scale roughness and dielectric constant rather than rocks. Taken Archimedes crater (29.7°N, 4.0°W; 83 km) as an example, there is a narrow halo (∼10 dB lower than background) just on its rim, which spatially correlates well with surface roughness calculated from Lunar Orbiter Laser Altimeter topography datasets (Fig. 1i). Dielectric constant can only make a difference of ∼0.4 dB in surface echo in this case, so apparently it is not the key factor for the dark halo. Therefore, LRS RDHC is more likely induced by surface roughness.

Conclusions: In this study, we examined the spatial distribution characteristics of the RDHCs in multi-band lunar radar images. RDHC has a more exogenetic origin compared to ODHC that is largely controlled by an endogenetic mechanism. Multiple evidences suggest that fine-grained material is the agent for radar dark halo, and that ODHC with a clearly volcanic origin can be a RDHC as well. LRS RDHC was surveyed for the first time and its low radar echo is most probably caused by surface roughness. More detailed investigation on RDHC is still ongoing and may help us to better understand the cratering mechanism and subsequent modifications of lunar surface.

References: [1] Ghent R. R. et al. (2005) *JGR*, doi: 10.1029 /2004JE002366. [2] Ghent R. R. et al. (2010) *Icarus, 209*, 818–835. [3] Schultz P. H. and Spudis P. D. (1979) *LPSC X*, 2899–2918. [4] Antonenko I. (2013) *LPSC XLIV*, Abstract #2607. [5] Le Feuvre M. and Wieczorek M. A. (2011) *Icarus, 214*, 1–20. [6] Bandfield J. L. et al. (2011) *JGR*, doi: 10.1029/2011JE003866. [7] Saunders R. S. and Wilhelms D. E. (1974) *USGS*. [8] Hawke B. R. and Bell J. F. (1981) *LPSC XII*, 665–678. [9] Kobayashi T. et al. (2012) *IEEE TGRS, 50*, 2161–2174.

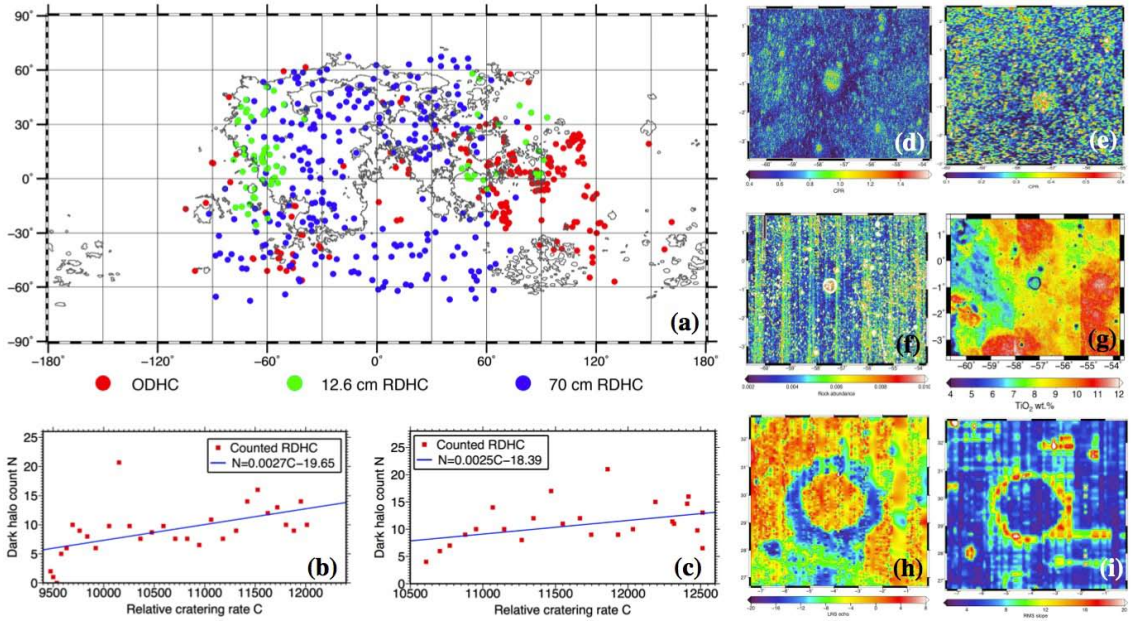

Figure 1. (a) Spatial distribution of 12.6 cm (green), 70 cm (blue) RDHCs and ODHCs (red). Numbers of 70 cm RDHCs versus cratering rate along longitude (b) and latitude (c). 12.6 cm (d) and 70 cm (e) radar images, rock abundance (f) and TiO_2 content (g) for Hermann crater (0.9°S, 57.3°W; 8 km). LRS surface echo (h) and RMS slope (i) for Archimedes crater (29.7°N, 4.0°W; 83 km).